8

Characterization of Nanotube-Reinforced Polymer Composites

Wenjie Wang[1] and N. Sanjeeva Murthy[2]
[1]*Ames Laboratory, Iowa State University, Ames, IA,*
[2]*New Jersey Center for Biomaterials, Rutgers – The State University of New Jersey, NJ U.S.A.*

1. Introduction

Polymers are more readily processible than metals and ceramics, but are not as strong or as stiff. But the mechanical attributes of the polymer can be significantly improved by reinforcing polymers with high Young's modulus fibers. The resulting polymer composites are an important class of light weight materials with excellent specific mechanical properties. Unlike micron size particles and short fibers used in conventional composites, carbon nanotubes (CNTs) allow polymers to be reinforced at the molecular level and thus impart significantly greater improvement in mechanical properties. This is because for the reinforcement to be effective, it is necessary that the fibers be sufficiently long and the interface between the fiber and the matrix be strong, features that are provided by CNTs. The advantages of polymer-nanotube composites (PNCs) were discussed by Calvert (Calvert, 1999). Besides the economic advantage brought about by mixing costly CNTs and inexpensive polymer matrices, it is possible that a synergy exists between the CNTs and polymer matrices so that it is possible to go beyond the simple rule of mixture, and make full use of CNTs' exceptional mechanical properties to enhance the mechanical properties of the composite.

There are several reviews of PNCs (e.g., Breuer & Sundararaj, 2004, Moniruzzaman & Winey, 2006, and Coleman et al., 2006). The present chapter is different from these excellent reviews in that it focuses on the structure and morphology of the reinforced structures, and the consequence of these structures to their performance. The general features of the PNCs will be further illustrated using the results from our work on the study of reinforcements in polyacrylonitrile (PAN) with multi- and single-wall carbon nanotubes (CNTs).

2. Polymer nanocomposites

2.1 Carbon nanotubes and nanofibers

Carbon nanotubes (CNTs), discovered by Iijima in 1991, are seamless cylinders made of rolled up hexagonal network of carbon atoms (Iijima, 1991). Single-wall nanotubes (SWNTs) consist of a single cylindrical layer of carbon atoms. The details of the structure of multi-wall carbon nanotubes (MWNTs) are still being resolved, but can be envisioned as a tubular structure consisting of multiple walls with an inter-layer separation of 0.34 nm. The diameter for inner most tube is on the scale of nanometer, and the length of the tube can be up to ~ μm. In one model, the MWNTs are considered as a single sheet of graphene that is

rolled up like a scroll to form multiple walls (Dravid et al., 1993). In another model, MWNT is thought to be made of co-axial walls consisting of hexagons aligned in helical manner, the individual tubes forming a nested-shell structure. Ge and Sattler (Ge & Sattler, 1993) found that as the graphene sheet rolls up and matches at joint line seamlessly, different wrapping angles resulting in different helicities is necessary for tubes to be separated by a uniform spacing. It is also likely that there could be the coexistence of scroll-type (open cylinder) and perfect Russian doll (nested shell) structures (Zhou et al., 1994). These two different structure models have an impact on the mechanical as well as the optical and electronic properties of CNTs. The carbon atoms in the plane of graphene sheet are bound with strong covalent sp^2 hybridized bonds. The interaction between walls can be approximated by weak van de Waals force or π bond. Thus, the sliding of walls with respect to each other might significantly reduce axial modulus of MWNT compared to SWNT, more so in the nested shell structure than in the scroll-type structure.

Vapor-grown carbon nano-fibers (VGCNF), which are also used as reinforcements, are 50-200 nm in diameter, 20-100 μm in length, and bear resemblance to MWNT, except that graphite sheets make an angle (~15°) to the long- axis (Uchida et al., 2006). Compared to the CNTs, VGCNF is less costly to produce.

CNTs have exceptional mechanical, optical, electrical and thermal properties (Chae et al., 2009; Chae et al., 2007; Guo et al., 2005; Koganemaru et al., 2004; Sreekumar et al., 2004; Ye et al., 2004). The elastic modulus of an isolated CNT, estimated using intrinsic thermal vibrations in TEM, is 1.8 TPa. (Treacy et al., 1996), almost an order of magnitude larger than that of carbon fibers. This axial modulus is higher than the 1 Tpa in-plane modulus of a single graphene sheet due to the wrap-up of the graphene sheet into a cylinder. Bower et al. measured the fracture strain of MWNT ≥18% in polymer composites, almost one or two orders of magnitude larger than carbon fibers (Bower et al., 1999). Chae and Kumar suggested that, because the tensile strength of CNTs is 100-600 GPa, about two orders of magnitude larger than that of ordinary carbon fibers, the CNTs might be the ultimate reinforcing materials for strong fibers (Chae & Kumar, 2009).

2.2 CNT/Polymer composites

The advantages of using CNTs as reinforcements in polymer matrices can be illustrated with the following empirical relationship between the critical length (l_c), and fracture stress σ_f of the reinforcing fiber (Wang et al., 2008a):

$$l_c = \frac{\sigma_f d}{2\tau_c} \tag{1}$$

where d is the fiber diameter, and τ_c is the interfacial strength. The critical fiber length is the minimum length of the fiber such that the failure occurs within the fiber, and thus ensures that it acts as an effective reinforcement. This relationship shows that nanotubes with their smaller diameter, and greater interfacial strength when molecularly dispersed serve as effective reinforcements even at smaller lengths.

The importance of bonding between CNTs and matrices for effective load transfer without slipping of contact surfaces has been widely recognized (Calvert, 1999). It is desirable that a large fraction of the load applied to the composites is efficiently transferred to CNTs through the interaction or bonding between the outer surface of the CNTs and the surrounding polymer matrix (Ajayan et al., 1997). It is widely accepted that larger the area of interface between the matrix and nano-fillers, the better the mechanical enhancement.

Several load-transfer models have been proposed and examined using atomistic molecular dynamic simulations. Most recent molecular dynamics simulations suggest that weak van der Waals force (Srivastava et al., 2003), as well as thermal expansion mismatch can contribute to strong interfacial interaction (Wong et al., 2003; Zhang & Wang, 2005). Panhuis's model suggests that the polymer chains will adapt their conformations to wrap around a single CNT (Panhuis et al., 2003; Wong et al., 2003). Frankland's model suggests that a small fraction of chemical bonds are formed between polymers and carbon atoms of the CNTs thus cross-links are formed between the matrix and CNTs (Frankland et al., 2002). Chemical bonding between CNT and polymer is apparent in the adhesion of polymers to CNT on the fracture surface through transmission electron microscopy (TEM) (Bower et al., 1999). However, Raman spectroscopy along with the SEM images of fracture surface by Ajayan et al. showed the sliding of SWNT bundles with respect to the matrix suggesting that the actual load transfer was poor between CNT and the polymer matrix, which rules out the chemical bonding model (Ajayan et al., 2000). A number of experiments have been carried out to test these models for the interaction between polymer matrix and CNTs (SWNTs and MWNTs) through tensile tests, microscopy and x-ray scattering. Deformation of the CNTs observed by x-ray scattering measurements (see section 3.3) shows an interaction between the matrix and CNTs that is sufficient to transfer the load from the matrix to the CNTs (Wang et al.,2008b). Actual measurements of the adhesion between the matrix and CNTs were also carried out using scanning probe microscope to pull out the CNTs from the matrix (Cooper et al., 2002). Coleman et al. found that a layer of polymer attached to the CNTs after pullout was very similar to the crystalline polymer coating nucleated by the MWNTs. The presence of interfacial crystalline layers partly contributes to the mechanical properties of composites (Coleman et al., 2006). Pull-out measurement can also be carried out by atomic force microscopy (AFM). Barber et al. attached one end of a single CNT to the tip of AFM and embedded the other end into the polymer matrix. The critical force needed to pull the nanotube from the polymer matrix was then recorded (Figure 1).

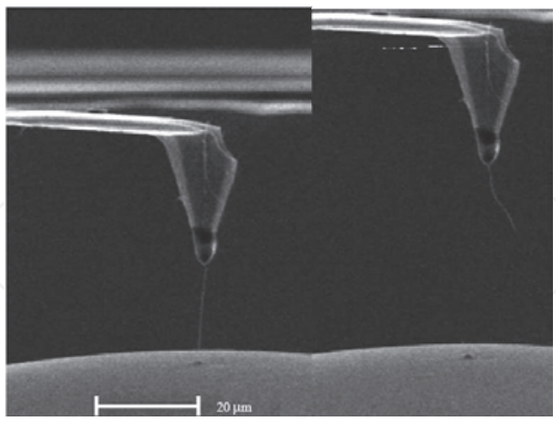

Fig. 1. Left panel shows that one end of a single CNT is attached to the AFM tip and the other is embedded in the solid polymer matrix. Right panel shows the process of pull-out of CNT. The critical force needed for pull-out can be recorded by AFM (Reprinted from Philosophical Transactions of the Royal Society A: Mathematical, Physical and Engineering Sciences, vol. 366, W. Wang, P. Ciselli, E. Kuznetsov, T. Peijs and A.H. Barber. "Effective reinforcement in carbon nanotube-polymer composites", Figure 2, Copyright 2008, with permission from the Royal Society.).

Because of the interfacial interaction between CNTs and the polymer matrix, the properties of the matrix in the interfacial regions are different from the bulk materials (Schadler, 2007). CNTs dispersed in the polymer matrix, despite the small volume fraction (usually 1-5 vol%), enhance the overall mechanical properties, also affect the structure of the matrix during conventional processing. Many observations show that the presence of CNTs can affect the crystallization behaviors of the polymers (Brosse et al., 2008; Grady et al., 2002; Liu et al., 2004) and alter the morphology of matrix (Brosse et al., 2008; Chatterjee et al., 2007). For instance, instead of the expected spherulites, crystalline lamellae were observed growing perpendicular to the surface of CNTs. (Brosse et al., 2008). Therefore, the microstructure of the polymer matrix should be taken into account when evaluating the performance of nanocomposites (Advani, 2006).
Two other factors that affect the performance of CNT-reinforced nanocomposites are the degree of dispersion and alignment of nanotubes. Poor or nonuniform dispersion causes the fillers to aggregate, acting as defect sites (Advani, 2006). Dispersion process is affected by interactions of CNT-CNT and CNT-matrix. It is controlled by several factors such as filler's size, specific surface area, and interfacial volumes (Moniruzzaman & Winey, 2006). The degree of dispersion of CNTs in polymer matrix can be assessed using small angle x-ray scattering as described in the following section. Rheological study of dispersions of MWNTs in the polymer matrix by Huang et al (Huang et al., 2006) also suggests that a satisfactory dispersion can be achieved if the mixing time exceeds a critical value (characteristic mixing time).

2.3 Processing of PNCs

CNTs are dispersed into the polymer matrix to form a polymer/CNTs composite, and there are several ways to achieve a good dispersion. Following is a condensed version of the various processing methods as discussed by Coleman et al. (Coleman et al., 2006). Solution processing is the easiest if the polymer can be dissolved in a suitable solvent. Typically, nanotubes well dispersed in a solvent is mixed with a polymer solution with energetic agitation (e.g., sonication), and the solvent is allowed to evaporate in a controlled way leaving a composite film. For insoluble thermoplastic polymers, the polymer is heated above either glass transition (if amorphous) or melt temperature (if semicrystalline) to form a viscous liquid, and the CNTs are mixed into this viscous liquid to be then processed into a fiber or a film using common production processes. For thermosetting polymers such as epoxy, the CNTs are blended when epoxy is in a liquid state, and the mixture is then allowed to cure. Chemical processing of Polymer/CNTs composites aims at formation of chemical bonds between the polymer matrix and the CNTs; this provides for stronger interaction between the polymer and CNTs and better dispersion, and thus results in better mechanical properties. Chemical methods include *in-situ* polymerization and functionalization of CNTs with polymer, also called polymer grafting.

3. Characterization of CNT/Polymer composites

Although the CNTs' high strength and stiffness as well as high aspect ratio promise significant improvement in mechanical properties of polymer nanocomposites (Treacy et al., 1996), the actual measured enhancement is below these expectations (Schaefer et al., 2003). The major reason might be the intrinsic van der Waals' attraction makes CNTs entangled agglomerates incapable of fully blending into the polymer matrix. Since the four

factors important to the reinforcement are CNTs' aspect ratio, alignment, dispersion, and interfacial interactions (Coleman et al., 2006), it is desirable to examine the morphology of CNTs in the polymer matrix. Several methods including x-ray diffraction, Raman spectroscopy, scanning and transmission electron microscopy are employed to characterize the structure, morphology and properties of carbon nanotube-reinforced polymer nanocomposites.

3.1 Electron microscopy

Transmission electron microscopy (TEM) and scanning electron microscopy (SEM) enable the visualization of the microscopic structure and morphology of CNTs in composites at resolution down to 0.1 nm (Michler, 2008; Sawyer et al., 2010). The limitations of using electron beam to probe the polymer are the low contrast (most polymers are made of light elements) and radiation damage. TEM is used to probe the bulk structure from thin sections of the material, and SEM to examine the surfaces. In addition to imaging, TEM is also used to carry out micromechanical measurements. Examples of these applications will be illustrated below.

3.1.1 Dispersion and alignment of the CNTs

One of the primary uses of microscopy is characterizing the dispersion and alignment of the nanotubes in the polymers. Figure 2a is an SEM image from a composite prepared by mixing aqueous solution poly(vinyl alcohol) with CNT dispersions followed by subsequent casting and controlled water evaporation (Shaffer & Windle, 1999). It shows homogeneous dispersion of the nanotubes even at 50 wt% loading. By examining the fracture surface using SEM, they confirmed the uniform dispersion of CNTs. Figure 2b shows the use of TEM to examine the dispersion of CNTs (Qian et al., 2000). In this experiment Qian et al. used high-energy sonication to disperse MWNTs (predispersed in toluene) into polystyrene (PS) dissolved in toluene, and the solvent was then evaporated to produce 0.4 mm thick films. Figure 2b shows 34 nm diameter MWNTs well dispersed down to the μm length scales. The inset is a plot of the loading of the CNT's at different length scale, and shows that homogeneity increases (decrease in standard deviation) with increase in the length scale. Furthermore, the TEM images also reveal defects that were present as a result of the polymer shrinkage primarily at the end of the nanotubes. Other than the quality of dispersion, both of these nanoscale images show that in PNCs, as pointed out by Fisher et al., the nanotubes are curved instead of being straight. Based on these observations, Fisher et al. illustrated that the reduction of effective modulus of CNT-reinforced materials is due to the curvature of embedded CNTs (Fisher et al., 2002).

Figure 3 illustrates the degree of alignment that can be achieved in PNC composites as seen in a TEM image (Thostenson & Chou, 2002). Unlike the two examples discussed above, in this instance, Thostenson & Chou extruded the polymer (polystyrene, PS) and a master batch of nanotube dispersed in PS using a micro-compounder. The film coming out of a rectangular die was drawn and solidified by passing over a chill roll. TEM was used to characterize the dispersion and alignment of MWNTs in polymer films. Figure 3a shows the large-scale dispersion and overall alignment of the carbon nanotubes and Figure 3b shows the alignment of the individual nanotubes. Examination of the drawn films showed that a draw ratio of five was sufficient to achieve a good nanotube alignment.

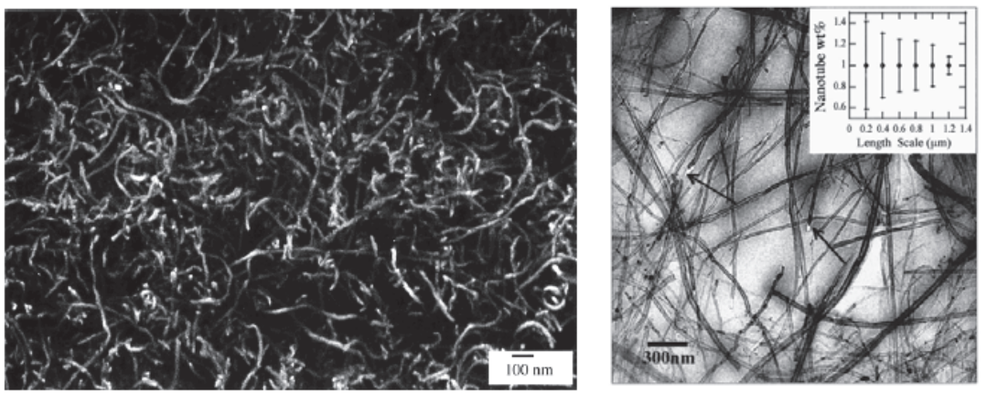

Fig. 2. Left Panel (a): A SEM image for 50 wt% CNT/ Poly(vinyl alcohol) composites (S.P. Shaffer and A.H. Windle, "Fabrication and characterization of carbon nanotube/poly(vinyl alcohol) composites". Advanced materials (1999). Vol. 11. 937-941. Copyright Wiley-VCH Verlag GmbH & Co. KGaA. Reproduced with permission.). Right panel (b): An example of TEM image at 1 μm length scale showing homogeneously dispersed MWNT in polystyrene (PS) matrix. Homogeneity of nanotube dispersion was evaluated by assessing the weight fraction of nanotubes in different areas in the TEM images for different length scale. The inset shows that homogeneity is greater at 1.2 μm length scale (small error bar) than lower length scale. An arrow in the image indicates the defects present at the nanotube ends (Reprinted with permission from D.Qian, E.C. Dickey, R. Andrews and T. Rantell., "Load transfer and deformation mechanisms in carbon nanotube-polystyrene composites", Applied Physics Letters, vol. 76, 2868-2870. Copyright 2000, American Institute of Physics.)

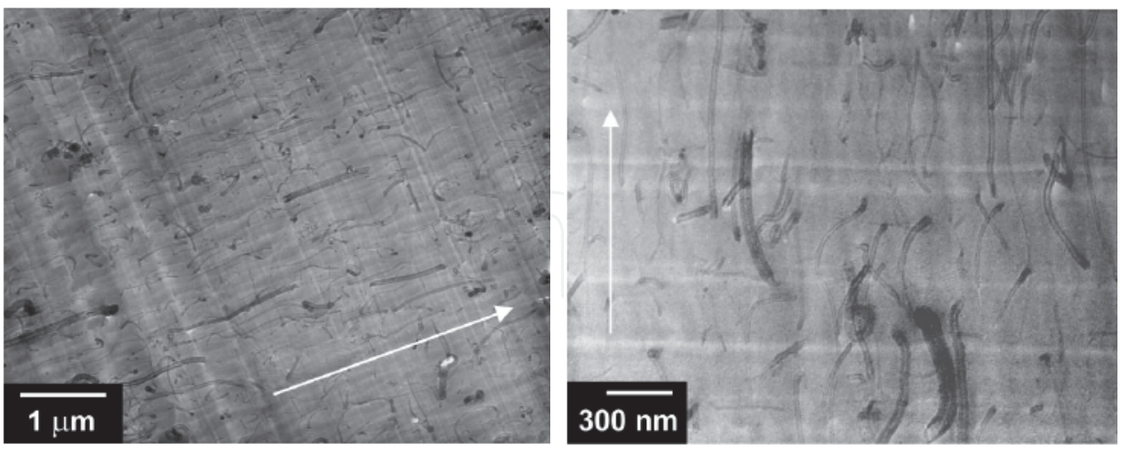

Fig. 3. TEM images of dispersion and alignment of CNTs in nanocomposites films. The arrows indicate flow/drawing direction. Left panel (a): TEM at length scale of micrometer. Right panel (b): TEM at length scale of nanometer (Reprinted with permission from E.T. Thostenson and T.W. Chou, "Aligned multi-walled carbon nanotube-reinforced composites: processing and mechanical characterization", J. Phys. D: Appl. Phys., vol. 35, L77-L80. Copyright 2002, Institute of Physics Publishing.).

3.1.2 Mechanical properties of CNTs

TEM is also used to measure the mechanical properties and to study the deformation mechanism in PNCs. In fact, the Young's modulus of CNTs, which is hard to measure by conventional means, was first directly measured using TEM from the thermal vibration amplitudes of CNTs, and thus confirming the predicted axial stiffness on the scale of terapascal (TPa) and the high axial strength due to the in-plane graphitic structure of CNTs (Treacy et al., 1996). Bower et al. (Bower et al., 1999) aligned MWNTs in the thermoplastic polymer (polyhydroxyaminoether, DowChemical Co.) films by stretching above the glass transition temperature and releasing the load at 300 K. The uniaxial alignment of MWNTs was confirmed by x-ray diffraction. The CNTs in the polymer matrix are bent (Figure 4), presumably because of the shrinkage of the polymer matrix as the composite is cooled from 100 °C to room temperature. The deformation was reversible at moderate bending, i.e. the CNTs returned to their straight cylindrical shape by heating the polymer matrix. Fracture surfaces in PNC's can be examined to ascertain the strength of the adhesion between the polymer and the nanotube. Figure 5 shows MWNT protruding from polymer matrix attached with a layer of polymer. All these observations point to the effective interactions and intimate contact between CNTs and polymer matrix. In a final example, Figure 6 shows the use of TEM to observe the nucleation and propagation of a crack induced in thin MWNT-PS film by thermal stresses in a TEM (Qian et al., 2000). The nucleation and propagation occur in regions of low CNT density and along the weak CNT-polymer interface. Also, the CNTs tend to align perpendicular to the crack and bridge the gap, and some of them are already pulled out, suggesting that the critical failure force is determined by interaction between polymer matrix and CNTs. These CNTs provide a closure force until a critical value is reached to be pulled out of the matrix.

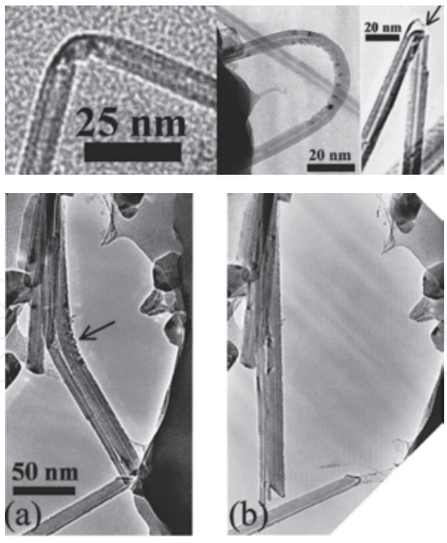

Fig. 4. Top panel: TEM images showing the buckling of in bent MWNTs in MWNT/polymer composites. Bottom panel: (a) A bent nanotube before heating; (b) the bent nanotube restored to its straight cylindrical shape after heating (Reprinted with permission from C. Bower, R. Rosen, L. Jin, J. Han and O. Zhou, "Deformation of carbon nanotubes in nanotube-polymer composites", Applied Physics Letters, vol. 74, 3317-3319. Copyright 1999, American Institute of Physics.).

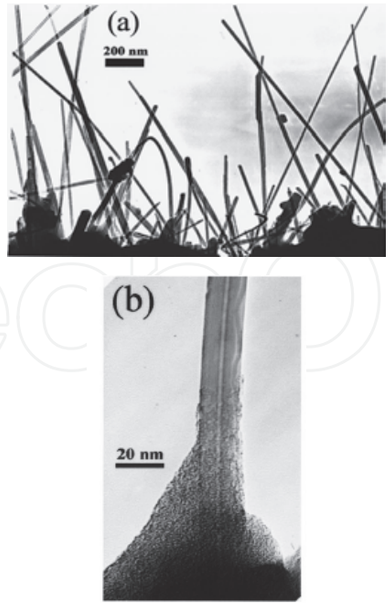

Fig. 5. TEM images of the fracture surface showing MWNT protruding from the polymer matrix suggestive of strong adhesion between the MWNT and the polymer matrix (Reprinted with permission from C. Bower, R. Rosen, L. Jin, J. Han and O. Zhou, "Deformation of carbon nanotubes in nanotube-polymer composites", Applied Physics Letters, vol. 74, 3317-3319. Copyright 1999, American Institute of Physics.).

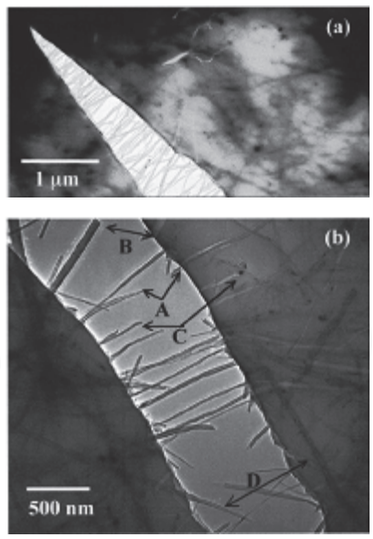

Fig. 6. Crack initiated by thermal stress. Upper panel shows the crack initiation and propagation at low CNT density areas. Lower panel shows the CNTs aligned perpendicular to the crack bridging the crack. Arrows labelled A, B, C and D point to CNTs that are broken and pulled out of matrix (Reprinted with permission from D. Qian, E.C. Dickey, R. Andrews and T. Rantell, "Load transfer and deformation mechanisms in carbon nanotube-polystyrene composites", Applied Physics Letters, vol. 76, 2868-2870. Copyright 2000, American Institute of Physics.).

3.2 Raman spectroscopy

Infrared (IR) and Raman spectroscopy (RS) are the two vibrational spectroscopic techniques widely used to obtain molecular structure information for the identification of polymers, functional groups and stereochemical structures. Both techniques measure the vibrational energies of molecules. However, for a vibrational motion to be IR active, the dipole moment of the molecule must change, and for a transition to be Raman active there must be a change in polarizability of the molecule. In most instances, IR and RS yield complementary information because IR activity suggests RS inactivity and vice versa. Sample requirements for RS are less stringent than for IR. Details of application of RS to CNTs have been discussed thoroughly in the literature (Dresselhaus et al., 2005), and a few examples of the use of RS to PNCs are provided here. For oriented specimen, the intensity of RS spectra line depends on the orientation of molecules relative to the polarization of the incident beam as well as scattering beam. This feature is used to determine the orientation distribution for CNTs in polymer matrix. Polarized RS has also been used to probe the one -dimensional nature of SWNT in the bulk materials (Gommans et al., 2000). These results show that the RS intensity has the same orientation dependence as nanotube's polarizability. A similar work on MWNT has also shown that there is a strong dependence of the graphite-like G band and the disorder-induced D band on the polarization geometry (Rao et al., 2000).

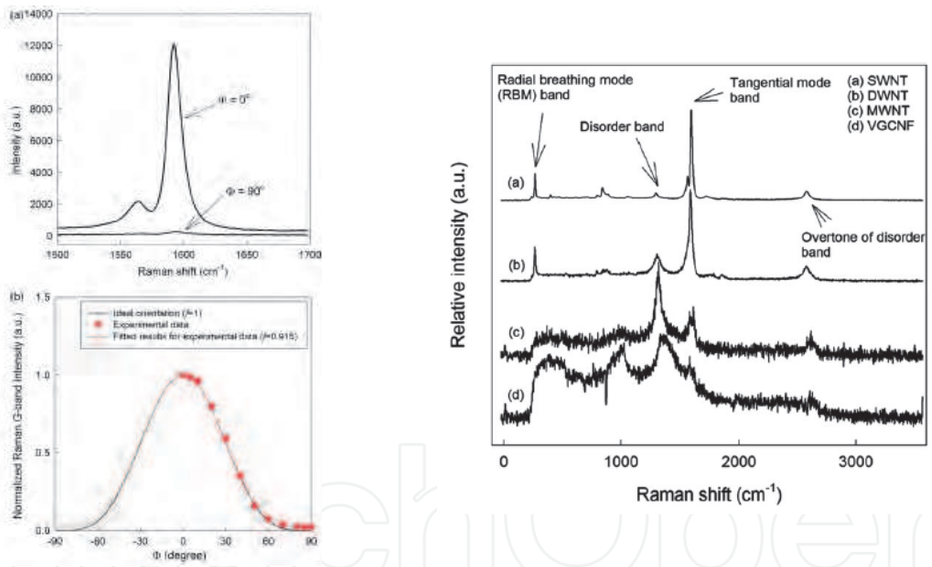

Fig. 7. Upper left panel: G-band Raman spectra for PAN/SWNT fiber. The ratio of the peak intensity at 1592 cm^{-1} are compared when the angles between polarizer and the fiber axis are 0 and 90°, respectively. Lower left panel: The normalized G-band Raman intensity as function of angles between polarizer and fiber axis. Experimental data are for PAN/SWNT (1 wt%) at draw ratio 51 (Reprinted from Polymer, Vol.47, H.G. Chae, M.L. Minus and S. Kumar, "Oriented and exfoliated single wall carbon nanotubes in polyacrylonitrile", 3494-4504. Copyright 2006, with permission from Elsevier.) Right panel: Raman spectra for pristine CNT powders (Reprinted from Polymer, Vol.46, H.G. Chae, T.V. Sreekumar, T. Uchida and S. Kumar, "A comparison of reinforcement efficiency of various types of carbon nanotubes in polyacrylonitrile fiber", 10925-10935. Copyright 2005, with permission from Elsevier.).

Mathematical description of Raman intensity distribution as a function of SWNT's orientation has been derived using Legendre polynomials by Liu et al. (Liu & Kumar, 2003). They built a relationship between 2nd and 4th orientation parameters of SWNT and Raman scattering intensity and depolarization ratio. This quantitative relation was used by Chae et al. to investigate the orientation of SWNT in polyacrylonitrile fibers (Chae et al., 2006). They measured G-band intensity ratio at about 1592 cm^{-1} for polarization parallel and perpendicular to the fiber axis (Figure 7). By comparing the G-band ratio for conventional spun and gel-spun PAN/SWNT fibers, they were able to conclude that the orientation of SWNT is only slightly improved by the gel-spinning process. They also showed that RS could be used to estimate the relative intensity of disorder band for SWNT, DWNT, MWNT, VGCNF (Chae et al., 2005) (Figure 7). They concluded that SWNT has best perfection while MWNT and VGCNF have more disorder (Chae et al., 2005).

3.3 X-ray scattering

X-ray scattering is an ideal tool to investigate the influence of CNTs on polymer morphology at multiple length scales from nm to sub μm length scales. This is achieved by using variations of the basic diffraction/scattering technique that are usually referred to as x-ray diffraction (XRD), wide-angle x-ray diffraction (WAXD), and small-angle x-ray scattering (SAXS). The scattering or diffraction intensity is expressed as a function of the scattering vector, $q(=4\pi\sin\theta/\lambda)$ or $s(=2\sin\theta/\lambda)$, 2θ being the scattering angle, and λ the x-ray wavelength. The sample preparation is far simpler than that for TEM. Whereas electron microscopy can provide information about the distribution of the CNTs and other structural information within a particular frame of an image, SAXS can provide similar data about the distribution, but averaged over lengths ~ mm in the bulk of the sample. Some of the characteristics of the PNCs that can be measured using x-ray scattering include the structural changes in the polymer due to the incorporation of the CNT, orientation of the polymer chains/crystals and the CNTs, and structure at the interface between the polymer and the CNT, and the changes in these features during deformation. The advent of synchrotron radiation, whose brilliance is ~ 10 orders of magnitude higher than that from a rotating anode tube, makes it possible to carry out *in-situ* dynamical measurements. Some of the data in this section were obtained from CNTs dispersed in polyacrylonitrile (PAN) that was then spun into a fiber. PAN fibers reinforced with CNTs are made by solution- or gel-spinning. PAN/CNTs fibers with significant enhancement in properties suggested good interactions between PAN and CNTs (Chae et al., 2006; Chae et al., 2005; Guo et al., 2005; Sreekumar et al., 2004; Uchida et al., 2006). These studies showed that the improvement in low strain is due to the interaction of PAN and CNTs, while the improvement as high strain is partly due to the CNT length.

3.3.1 Characterization of the CNTs

Before discussing the results for the PNCs, we will first discuss some of the scattering data relevant to the characterization for the CNTs. Historically, the MWNTs were observed by electron microscopy and were depicted as concentric seamless cylinders (Iijima, 1991). This model was used to interpret XRD data (Pasqualini, 1997), and further direct evidence appeared later to support this concentric cylinder model (Xu et al., 2001). However, there has been evidence that suggest that the local structure is similar to turbostratic graphite or scrolls of graphite sheets (Dravid et al., 1993; Zhou et al., 1994). More recent data suggest that while thin MWNTs could be modelled as concentric 7-15 tubules, thicker MWNTs were

found to be mixtures of both scroll-type MWNT and concentric-cylinder (nested Russian doll) MWNTs (Maniwa et al., 2001).

An individual CNT cannot be characterized using SAXS. However, due to the π-π chemical bonding and van de Waals interactions, the CNTs tend to aggregate into bundles while lacking a clear-cut rod-like morphology (Schaefer et al., 2003a), and this typical morphology can be characterized using SAXS. Schaefer et al. combined small-angle light scattering, ultra-SAXS and SAXS to measure morphology and degree of dispersion of SWNTs and MWNTs suspended in water (Schaefer, 2003a; Schaefer, 2003b). They found that the intensities over 5 decades of q are characterized by different power laws. The power-law of intensity from SWNT indicates a branched rope network with fractal characteristics. Porod's law was observed at length scale smaller than inner radius, suggesting the smoothness of interface. The nonuniform dispersion of CNTs in polymers partly explains why the reinforcement of CNTs to polymer composites falls below expectations.

In another experiment (Inada et al., 2005), two segments of different power-law behavior were observed in the intensity distribution (Figure 8). One segment conforms to Porod's law corresponding to smooth interfaces. The other follows a power-law with exponent -1, suggesting scattering is from a rod-like structure. The scattering could be modeled as those from MWNTs represented as hollow tubes with an inner diameter of about 8 nm and a wall thickness of 6 nm, which is in agreement with the reported results from direct measurement through TEM.

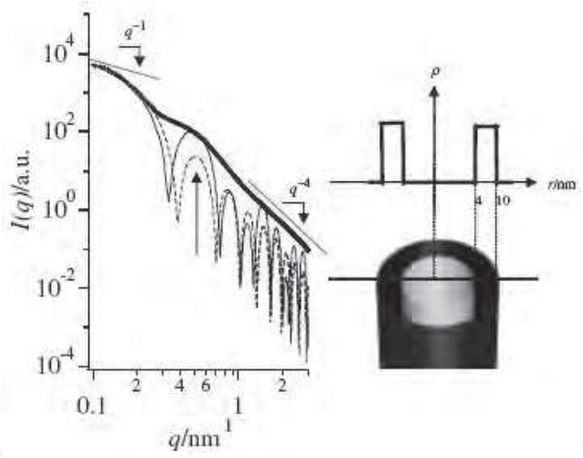

Fig. 8. Left: Measured SAXS intensity as function of scattering vector. Two power laws were presented indicating a one-dimension cylinder structure and sharp interface, respectively. Straight line and dotted line are calculated for a core-shell and hard cylinder models, respectively. Right: The best fit parameter suggest the structure of CNT is a core-shell structure (Reprinted from T. Inada et al., "Small-angle x-ray scattering from multi-wall carbon nanotubes (CNTs) dispersed in polymeric matrix", Chemistry Letters, Vol. 34, 525 (2005), with permission from The Chemical Society of Japan.)

3.3.2 SAXS characterization of the voids and the CNTs in the polymer

Voids are invariably formed in the fibers during the spinning and the drawing process, especially in the presence of reinforcements. Voids, and in general any scattering entities, give rise to SAXS that can be analyzed to obtain information about the length, diameter, and

orientation of these entities as well the information about the nature of the interface. In the work with PAN fibers, the degree of orientation of the voids measured by SAXS was found to be same as those of the crystalline domains observed in WAXS. Both increased reversibly upon stretching, indicating that the voids are integral parts of the polymer matrix and closely associated with the crystalline domains in the fibrils (Wang et al., 2009). SAXS data also showed large changes in the size distribution of the voids during elongation in the solution spun PAN fibers, but not the composite fibers. Furthermore, heating the fiber above the glass transition temperature (T_g) decreased the volume fraction of the voids considerably as indicated by a decrease in the scattered intensity. Figure 9 shows examples of the decay in equatorial scattering with scattering angle. The rate of this decay, as indicated by the slope of the log-log plot (called the exponent) provides valuable insight into the nature of the void-polymer interface. In the plot of the PAN with MWNT, we see the exponent is 4.4 (Figure 9a). An exponent of 4.0 would indicate a sharp, smooth interface. A value higher than 4 suggests that in the PAN/MWNT sample, there is a diffuse interface between the polymer and the void as indicated schematically in the figure. An exponent between 3 and 4 would indicate a rough void-polymer interface, which was observed in gel-spun fibers without any CNT's (Figure 9b). An exponent between 2 and 3 indicates that the structure within the void is similar to a mass-fractal. It is speculated that because of the nature of gel-spinning process, the voids are partially filled with polymer, and perhaps CNT, and as a result the scattering exponent falls below 3 as indicated in Figure 9c. It is possible that a similar analysis can be carried out to probe the nanotube-polymer interface provided there is a contrast between the CNTs and the matrix.

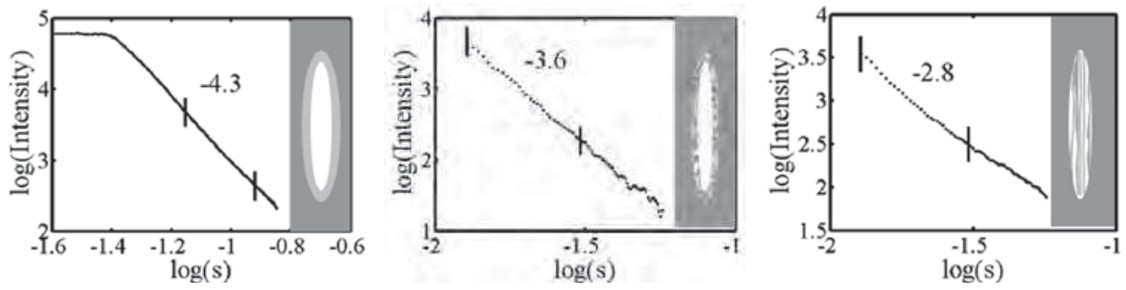

Fig. 9. Power law for equatorial intensities. (a) PAN/MWNT for a void with diffuse boundary ; (b) gel-spun PAN for a void with surface fractal; (c) gel-spun PAN/SWNT for a void with mass fractal The linear segments that are fitted to obtain the fractal dimension are shown in the figure (Wang et al., 2009).

3.3.3 WAXD analysis of the polymer and the CNTs

Figure 10 shows example of the 2D diffraction patterns and the corresponding 1D scans that can be obtained from polymer composites with CNTs. Because of the large fraction of the polymer (95%) the major features in these scans are due to the polymer, and these features can be used to follow the changes in the polymer structure in terms of the unit cell dimensions, crystallinity, crystallite size and polymer orientation (Wang et al., 2008b). For example, the data show that a monotonic decrease in PAN inter-chain spacing with the fiber strain is accompanied by a reversible change from helix to zigzag conformation, and by changes in the axial repeats of the two conformations. These changes are much larger in gel-spun fibers than in solution-spun fibers, indicating more effective load transfer between the

amorphous and crystalline segments in gel -spun fibers. In addition to the intense polymer peaks, it is also possible to see the weak features of the CNT reinforcements in the pattern, especially in the 1D scans. Note the broad feature due to MWNT in Figure 10e, and the sharp features due to VGCNF in Figure 10f. The changes in these features with stress were used to ascertain the modulus of the polymer and the CNT in the composite. Such data are potentially useful in determining the distribution of load between the two components.

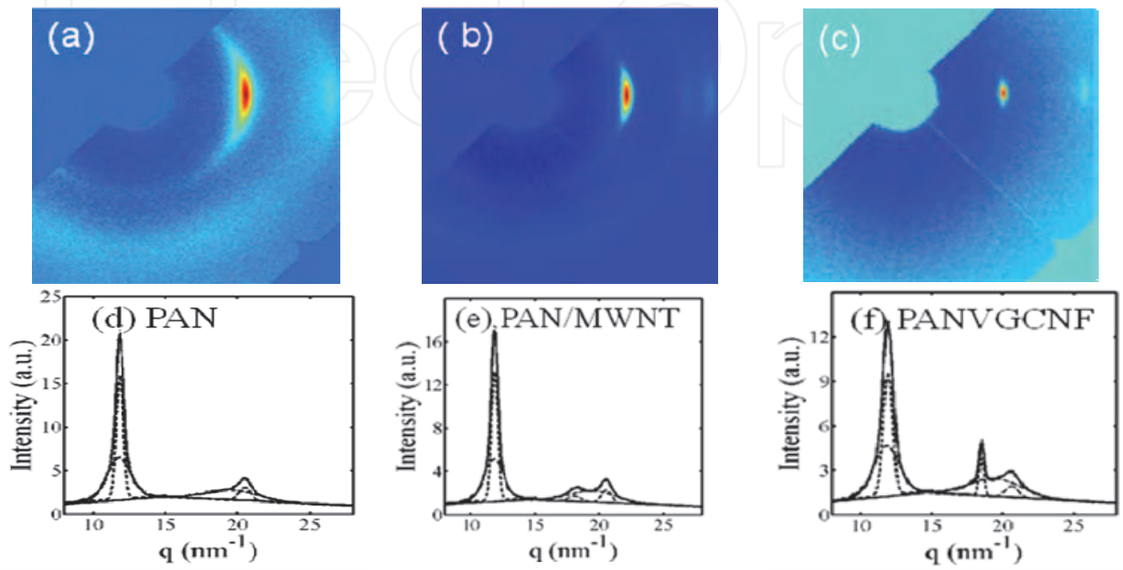

Fig. 10. Upper Panel: Two dimensional wide-angle x-ray diffraction pattern for (a) solution-spun PAN ; (b) solution-spun PAN/MWNT; (c) gel-spun PAN/SWNT fibers. Lower Panel: Profile fitted equatorial scans: (d) PAN; (e) PAN/MWNT; (f) PAN/VGCNF. The data for gel fibers are similar to that of PAN. (Reprinted from Polymer, Vol.49, W. Wang, N.S. Murthy, H.G. Chae and S. Kumar, "Structural changes during deformation in carbon nanotube-reinforced polyacrylonitrile fibers", 2133-2145. Copyright 2008, with permission from Elsevier.)

3.3.4 Alignment of the CNTs and the polymer

As indicated earlier, to a large extent, the strength, modulus and shrinkage properties of the polymer composite are determined by the distribution in orientation and alignment of both the CNT and the polymer. XRD is an appropriate tool for determining this parameter. (Wang et al., 2008b). For instance, Pichot et al. obtained the orientation of SWNT and PVA chain by azimuthal intensity distribution (Pichot et al., 2006). They related the alignment of SWNT in polyvinyl alcohol (PVA) fibers with different draw ratio and accounted for the improvement of alignment with draw ratio by applying a simplistic continuum mechanical model, i.e. the induced alignment is due to the constant volume. In the work on PAN fibers, by measuring the orientation during loading and unloading of the fibers, it was found that the orientation reversibly increases as the fiber is stressed (Wang et al., 2008b).

Chen et al. (Chen et al., 2006) employed in-situ WAXS/SAXS to investigate the deformation of nanocomposites fiber containing fluorinated MWNT (FMWNT) and fluorinated polyethylene-propylene. Orientation of FMWNT can be characterized by (002) reflection of

WAXS and quantitatively described by Hermans' orientation parameter. Similar experiments were carried out by Wang et al. (Wang et al., 2008b) on the deformation of PAN and its nanocomposites containing a variety of CNTs (MWNT,VGCNF,SWNT). The effect of CNT reinforcement could be ascertained by monitoring the structural change in PAN crystals. In this work, it was found that CNTs facilitate the orientation of the PAN crystals during deformation (Figure 11) and increase the load-transferred to PAN crystals as evidenced by their increased lateral and axial strain at 75 ^{o}C.

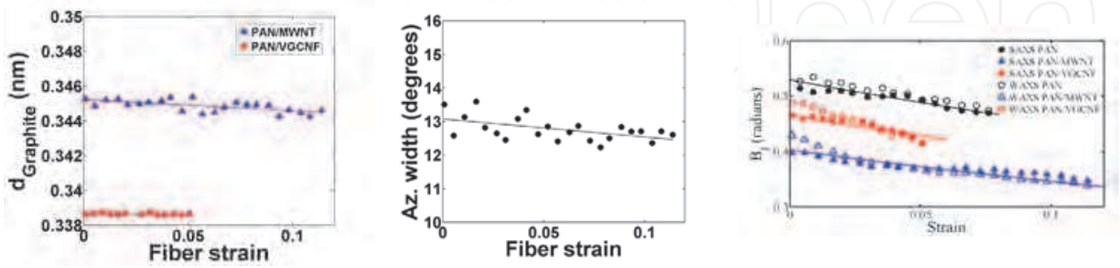

Fig. 11. (a)-(c) from left to right. Changes in the *d*-spacing of carbon as a function of strain derived from the Bragg's peak of nanotubes at room temperature; (b) Degree of orientation of MWNT in the form of the azimuthal breadth.(Reprinted from Polymer, Vol.49, W. Wang, N.S. Murthy, H.G. Chae and S. Kumar, "Structural changes during deformation in carbon nanotube-reinforced polyacrylonitrile fibers", 2133-2145. Copyright 2008, with permission from Elsevier.) (c) Changes in the extent of misorientation (B_f) for scattering entities at room temperature. Black circle, blue triangle and red square represent PAN, PAN/MWNT, and PAN/VGCNF, respectively. Filled and empty symbols represent SAXS and WAXS results, respectively. Straight line segments are calculated based on affine deformation model. (Wang et al.,. 2009).

3.3.5 Deformation of the CNTs in the composite

The diffraction patterns shown in Figure 10 can be used to characterize the deformation of CNTs under stress by monitoring the changes in the (002) peak of CNTs. This interlayer distance d_{002} is used to ascertain the changes in the lattice dimension under strain (Figure 11). This figure also shows the changes in the azimuthal width of these reflections with strain as well as the crystallite size corresponding to this reflection. The changes in these parameters show that CNTs deform under load and thus contributes to the increased modulus, and also alter the response of the PAN matrix to stress, thus enhancing the performance of the composite.

4. Conclusions

Among the many techniques that are currently available, electron microscopy, Raman spectroscopy and x-ray scattering have proved to be most valuable to study the structure in polymer nanocomposites. These techniques complement each other by covering overlapping length scales from sub nm to μm. These techniques are valuable in assessing the dispersion, alignment of the nanotubes in the matrix, to probe the adhesion and the interface between the nanotube and the polymer, and to study the structural changes that occur due to the interaction between the two components as well as during deformation.

5. References

Advani, S. G. (2006). Processing and Properties of Nanocomposites: World Scientific.

Ajayan, P. M., Redlich, P., & Ruhle, M. (1997). Structure of carbon nanotube-based nanocomposites. Journal of Microscopy, 185, 275-282.

Ajayan, P. M., Schadler, L. S., Giannaris, C., & Rubio, A. (2000). Single-Walled Carbon Nanotube-Polymer Composites: Strength and Weakness. Advanced Materials, 12(10), 750-753.

Bower, C., Rosen, R., Jin, L., Han, J., & Zhou, O. (1999). Deformation of carbon nanotubes in nanotube-polymer composites. Applied Physics Letters, 74(22), 3317-3319.

Breuer, O., & Sundararaj, U. (2004). Big Return From Small Fibers: A Review of Polymer/Carbon Nanotube Composites. Polymer Composites, 25(6), 630-645.

Brosse, A.-C., Tence-Girault, S., Piccione, P. M., & Leibler, L. (2008). Effect of multi-walled carbon nanotubes on the lamellae morphology of polyamide-6. Polymer, 49, 4680-4686.

Calvert, P. (1999). Nanotube composites: A recipe for strength. Nature, 399, 210-211.

Chae, H. G., Choi, Y. H., Minus, M. L., & Kumar, S. (2009). Carbon nanotube reinforced small diameter polyacrylonitrile based carbon fiber. Composites Science and Technology, 69, 406-413.

Chae, H. G., & Kumar, S. (2009). Making Strong Fibers. Science, 319(5865), 908-909.

Chae, H. G., Minus, M. L., & Kumar, S. (2006). Oriented and exfoliated single wall nanotubes in polyacrylonitrile. Polymer, 47(10), 3494-3504.

Chae, H. G., Minus, M. L., Rasheed, A., & Kumar, S. (2007). Stabilization and Carbonization of gel spun polyacrylonitrile/single Wall nanotube Composite Fibers. Polymer, 48, 3781-3789.

Chae, H. G., Sreekumar, T. V., Uchida, T., & Kumar, S. (2005). A comparison of reinforcement efficiency of various types of carbon nanotubes in polyacrylonitrile fiber. Polymer, 46, 10925-10935.

Chatterjee, T., Mitchell, C. A., Hadjiev, V. G., & Krishnamoorti, R. (2007). Hierarchical Polymer-Nanotube Composites. Advanced Materials, 19, 3850-3853.

Chen, X., Burger, C., Fang, D., Sics, I., Wang, X., He, W., et al. (2006). In-Situ X-ray Deformation Study of Fluorinated Multiwalled Carbon Nanotube and Fluorinated Ethylene-Propylene Nanocomposite Fibers. Macromolecules, 39, 5427-5437.

Coleman, J. N., Khan, U., & Gun'ko, Y. K. (2006). Mechanical Reinforcement of Polymers Using Carbon Nanotubes. Advanced Materials, 18, 689-705.

Cooper, C. A., Cohen, S. R., Barber, A. H., & Wagner, H. D. (2002). Detachment of nanotubes from a polymer matrix. Applied Physics Letters, 81(20), 3873-3875.

Dravid, V. P., Lin, X., Wang, Y., Wang, X. K., Yee, A., Ketterson, J. B., et al. (1993). Buckytubes and Derivatives: Their Growth and Implications for Buckyball Formation. Science, 259(5101), 1601-1604.

Dresselhaus, M. S., Dresselhaus, G., Saito, R., & Jorio, A. (2005). Raman spectroscopy of carbon nanotubes. Physics Reports, 409, 47-99.

Fisher, F. T., Bradshaw, R. D., & Brinson, L. C. (2002). Effects of nanotube waviness on the modulus of nanotube-rein. Applied Physics Letters, 80, 4647--4649.

Frankland, S. J. V., Caglar, A., Brenner, D. W., & Griebel, M. (2002). Molecular Simulation of the Influence of Chemical Cross-Links on the Shear Strength of Carbon Nanotube-Polymer Interfaces. J. Phys. Chem. B, 106, 3046-3048.

Ge, M., & Sattler, K. (1993). Vapor-Condensation Generation and STM Analysis of Fullerene Tubes. Science, 260(5107), 515-518.

Gommans, H. H., Alldredge, J. W., Tashiro, H., Park, J., Magnuson, J., & Rinzler, A. G. (2000). Fibers of aligned single-walled carbon nanotubes: Polarized Raman spectroscopy. Journal of Appied Physics, 88, 2509-2514.

Grady, B. P., Pompeo, F., Shambaugh, R. L., & Resasco, D. E. (2002). Nucleation of Polypropylene Crystallization by Single-Walled Carbon Nanotubes. Journal of Physical Chemistry B, 106, 5852-5858.

Guo, H., Sreekumar, T. V., Liu, T., Minus, M., & Kumar, S. (2005). Structure and Properties of Polyacrylonitrile/single wall carbon nanotube composite films. Polymer, 46, 3001-3005.

Huang, Y. Y., Ahir, S. V., & Terentev, E. M. (2006). Dispersion rheology of carbon nanotubes in a polymer matrix. Physical Review B, 73, 125422.

Iijima, S. (1991). Helical microtubules of graphitic carbon. Nature, 354, 56-58.

Inada, T., Masunaga, H., Kawasaki, S., Yamada, M., Kobori, K., & Sakurai, K. (2005). Small-angle X-ray Scattering from Multi-walled Carbon Nanotubes (CNTs) Dispersed in Polymeric Matrix. Chemistry Letters, 34(4), 524-525.

Koganemaru, A., Bin, Y., Agari, Y., & Matsuo, M. (2004). Composites of Polyacrylonitrile and Multiwalled Carbon Nanotubes Prepared by Gelation/Crystallization from solution. Advanced Functional Materials, 14(9), 842-850.

Liu, T., & Kumar, S. (2003). Quantitative characterization of SWNT orientation by polarized Raman spectroscopy. Chemical Physics Letters, 378, 257-262.

Liu, T., Phang, I. Y., Shen, L., Chow, S. Y., & Zhang, W.-D. (2004). Morphology and Mechanical Properties of Multiwalled Carbon Nanotubes Reinforced Nylon-6 Composites. Macromolecules, 37, 7214-7222.

Maniwa, Y., Fujiwara, R., Kira, H., Tou, H., Nishibori, E., Takata, M., et al. (2001). Multiwall carbon nanotubes grown in hydrogen atmosphere: An X-ray study. Physical Review B, 64, 073105-073104.

Michler, G. H. (2008). Electron Microscopy of Polymers (1st ed.): Springer.

Moniruzzaman, M., & Winey, K. I. (2006). Polymer Nanocomposites Containing Carbon Nanotubes. Macromolecules, 39, 5194-5205.

Panhuis, M. i. h., Maiti, A., Dalton, A. B., Noort, A. v. d., Coleman, J. N., McCarthy, B., et al. (2003). Selective Interaction in a Polymer-Single-Wall Carbon Nanotube Composite. J. Phys. Chem. B, 107, 478-482.

Pasqualini, E. (1997). Concentric carbon structure. Physical Review B, 56(13), 7751-7754.

Pichot, V., Badaire, S., Albouy, P. A., Zakri, C., Poulin, P., & Launois, P. (2006). Structural and mechanical properties of single-wall carbon nanotube fibers. Physical Review B, 74(245416), 245416.

Qian, D., Dickey, E. C., Andrews, R., & Rantell, T. (2000). Load Transfer and deformation mechanisms in carbon nanotube-polystyrene composites. Applied Physics Letters, 76(20), 2868-2870.

Rao, A. M., Jorio, A., Pimenta, M. A., Dantas, M. S. S., Saito, R., Dresselhaus, G., et al. (2000). Polarized Raman Study of Aligned Multiwalled Carbon Nanotubes. Physical Review Letters, 84, 1820-1823.

Sawyer, L., Grubb, D. T., & Meyers, G. F. (2010). Polymer Microscopy (3rd ed.): Springer.

Schadler, L. (2007). Nanocomposites: Model Interface. Nature Materials, 6, 257-258.

Schaefer, D. W., Brown, J. M., Anderson, D. P., Zhao, J., Chokalingam, K., Tomlin, D., et al. (2003a). Structure and dispersion of carbon nanotubes. J. Appl. Cryst., 36, 553-557.

Schaefer, D. W., Zhao, J., Brown, J. M., Anderson, D. P., & Tomlin, D. W. (2003b). Morphology of dispersed carbon single-walled nanotubes. Chemical Physics Letters, 375, 369-375.

Shaffer, M. S. P., & Windle, A. H. (1999). Fabrication and characterization of carbon nanotube/poly(vinyl alcohol) composites. Advanced Materials, 11, 937-941.

Sreekumar, T. V., Liu, T., Min, B. G., Guo, H., Kumar, S., Hauge, R. H., et al. (2004). Polyacrylonitrile Single-Walled Carbon Nanotube Composite Fibers. Advanced Materials, 16(1), 58-61.

Srivastava, D., Wei, C., & Cho, K. (2003). Nanomechanics of carbon nanotube and composite. Appl. Mech. Rev 56(2), 215-230.

Thostenson, E. T., & Chou, T.-W. (2002). Aligned multi-walled carbon nanotube-reinforced composites: processing and mechanical characterization. J. Phys. D: Appl. Phys., 35, L77-L80.

Treacy, M. M. J., Ebbesen, T. W., & Gibson, J. M. (1996). Exceptionally high Young's modulus observed for individual carbon nanotubes. Nature, 381, 678-680.

Uchida, T., Anderson, D., Minus, M., & Kumar, S. (2006). Morphology and modulus of vapor grown carbon nano fibers Journal of Materials Science, 41(18), 5851-5856.

Wang, W., Ciselli, P., Kuznetsov, E., Peijs, T., & Barber, A. H. (2008a). Effective reinforcement in carbon nanotube-polymer composites. Philosophical Transactions of the Royal Society A: Mathematical, Physical and Engineering Sciences, 366, 1613-1626.

Wang, W., Murthy, N. S., Chae, H. G., & Kumar, S. (2008b). Structural changes during deformation in carbon nanotube-reinforced polyacrylonitrile fibers. Polymer, 49(8), 2133-2145.

Wang, W., Murthy, N. S., Chae, H. G., & Kumar, S. (2009). Small-Angle X-ray Scattering Investigation of Carbon Nanotube-Reinforced Polyacrylonitrile Fibers During Deformation. Journal of Polymer Science: Part B: Polymer Physics.

Wong, M., Paramsothy, M., Xu, X. J., Ren, Y., Li, S., & Liao, K. (2003). Physical interactions at carbon nanotube-polymer interface. Polymer, 44, 7757-7764.

Xu, G., Feng, Z.-c., Popovic, Z., Lin, J.-y., & Vittal, J. J. (2001). Nanotube structure Revealed by High-resolution X-ray Diffraction. Advanced Materials, 13(4), 264-267.

Ye, H., Lam, H., Nick, T., Gogotsi, Y., & Frank, K. (2004). Reinforcement and rupture behavior of carbon nanotubes-polymer nanofibers. Applied Physics Letters, 85(10), 1775-1777.

Zhang, Y. C., & Wang, X. (2005). Thermal effects on interfacial stress transfer characteristics of carbon nanotubes/polymer composites. International journal of solids and structures, 42, 5399-5412.

Zhou, O., Fleming, R. M., Murphy, D. W., Chen, C. H., Haddon, R. C., Ramirez, A. P., et al. (1994). Defects in Carbon Nanostructure. Science, 263, 1744-1747.

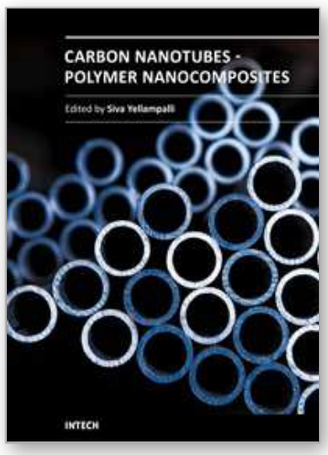

Carbon Nanotubes - Polymer Nanocomposites

Edited by Dr. Siva Yellampalli

ISBN 978-953-307-498-6
Hard cover, 396 pages
Publisher InTech
Published online 17, August, 2011
Published in print edition August, 2011

Polymer nanocomposites are a class of material with a great deal of promise for potential applications in various industries ranging from construction to aerospace. The main difference between polymeric nanocomposites and conventional composites is the filler that is being used for reinforcement. In the nanocomposites the reinforcement is on the order of nanometer that leads to a very different final macroscopic property. Due to this unique feature polymeric nanocomposites have been studied exclusively in the last decade using various nanofillers such as minerals, sheets or fibers. This books focuses on the preparation and property analysis of polymer nanocomposites with CNTs (fibers) as nano fillers. The book has been divided into three sections. The first section deals with fabrication and property analysis of new carbon nanotube structures. The second section deals with preparation and characterization of polymer composites with CNTs followed by the various applications of polymers with CNTs in the third section.

INTECH
open science | open minds

InTech Europe
University Campus STeP Ri
Slavka Krautzeka 83/A
51000 Rijeka, Croatia
Phone: +385 (51) 770 447
Fax: +385 (51) 686 166
www.intechopen.com

InTech China
Unit 405, Office Block, Hotel Equatorial Shanghai
No.65, Yan An Road (West), Shanghai, 200040, China
中国上海市延安西路65号上海国际贵都大饭店办公楼405单元
Phone: +86-21-62489820
Fax: +86-21-62489821

IntechOpen